

# Chapter 4

## Decontamination of Magnesium Slag



**Abstract** Magnesium slag is a valuable resource when proper disposal and utilization are adopted. The main pollution of magnesium slag caused are dust pollution and fluorine pollution. Formation mechanism of fine magnesium slag dust is investigated. Alike steel slag, phase transition of dicalcium silicate in magnesium slag around 500 °C brings volume expansion, which causes the disintegration and powdering of magnesium slag. Chemical stabilization experiments of the slag were carried out. The effects of phosphorus compounds, boron compounds and rare earth oxides doping on stabilization of magnesium slag was discussed. Catalytic action of calcium fluoride on magnesium smelting was revealed. Fluoride-free mineralizers for magnesium smelting were tested in industrial scale.

**Keywords** Magnesium slag · Dust pollution · Volume expansion · Chemical stabilization · Phase transition

### 4.1 Fixation of Magnesium Slag Dust

#### 4.1.1 Formation Mechanism of Fine Magnesium Slag Dust

When the Pidgeon process is used to smelt metallic magnesium, crude magnesium ingots are removed after the reduction reaction is complete; meanwhile, magnesium slag is discharged from the reduction tank. The magnesium slag is transported to a slag yard and then cooled naturally to room temperature. The temperature of magnesium smelting is 1200 °C, and so, magnesium slag is also at this temperature before it leaves the reduction retort. When hot pellet-shaped magnesium slag is discharged and transported to a slag yard, it becomes a fine powdery magnesium slag after cooling and weathering. Sometimes, to accelerate the cooling and to increase the turnover rate of a slag yard, water is poured on the hot magnesium slag pile to accelerate the cooling process.

In studying the phase transformation of dicalcium silicate ( $\text{Ca}_2\text{SiO}_4$ ,  $\text{C}_2\text{S}$ ) in steel slag, scientists discovered that  $\text{C}_2\text{S}$  has five crystal forms, namely  $\alpha$ -,  $\alpha'_\text{H}$ -,  $\alpha'_\text{L}$ -,  $\beta$ -, and  $\gamma$ - $\text{C}_2\text{S}$ . Among these phases, the  $\beta$  phase is a monoclinic system that is a stable phase at high temperature and a metastable phase at normal temperature; the  $\gamma$  phase

is an orthorhombic system that is a stable phase at normal temperature. When the temperature changes from high to low,  $C_2S$  undergoes several phase transitions; one involves a 12–14% expansion in volume when the  $\beta$ - $C_2S$  phase converts to the  $\gamma$ - $C_2S$  phase in the range of 675–490 °C [1–3]. The phase transition diagram of  $C_2S$  is shown in Fig. 4.1 [1]. The phase transition phenomenon of magnesium slag is similar to that of steel slag.  $CaO$  and  $SiO_2$  accounting for 70–90% of magnesium slag and can form  $\beta$ - $C_2S$  at a smelting temperature of 1200 °C inside a reduction retort. During a slow natural cooling process,  $\beta$ - $C_2S$  transforms into  $\gamma$ - $C_2S$  in the range of 500–700 °C, and this is accompanied by a volume expansion. Such a volume expansion causes the disintegration and powdering of magnesium slag, and this causes pellet-shaped magnesium slag to turn into powder.

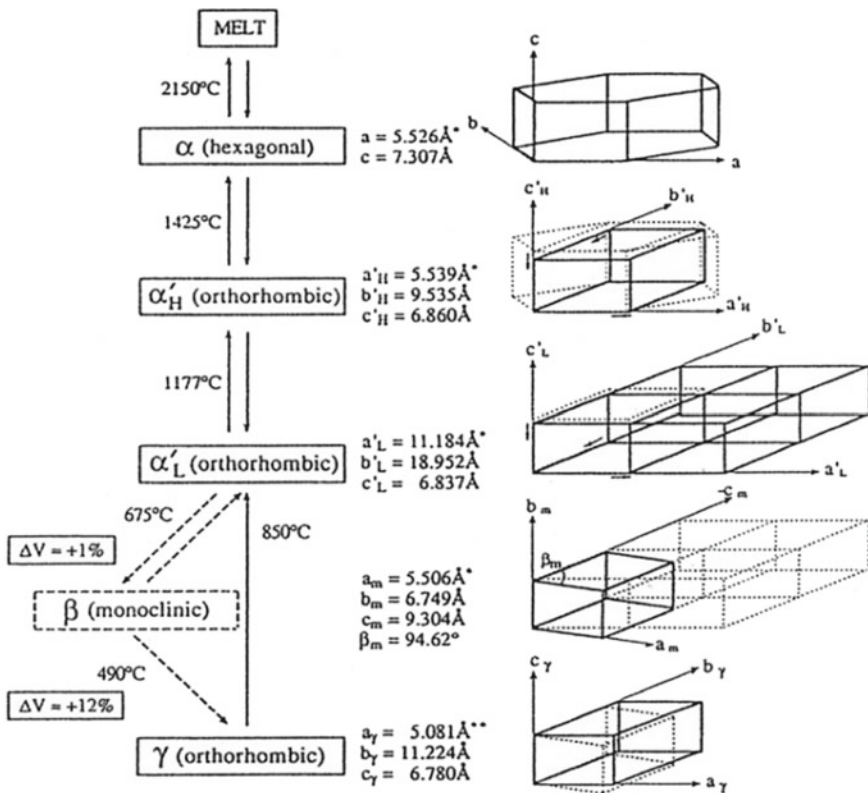


Fig. 4.1 Phase transition diagram of  $C_2S$  (Reprinted from Ref. [1] Copyright 1992, with permission from John Wiley and Sons)

### 4.1.2 Volume Stability of Magnesium Slag

The volume stability of magnesium slag is an important factor that affects the recycling and utilization of magnesium slag. If building materials that contain magnesium slag expand and crack in a later stage, it will seriously affect the use of the materials. Therefore, similar to that of steel, the volume stability problem of magnesium slag has attracted the attention of researchers at home and abroad. Before the phase transition, magnesium slag is in the shape of egg-sized pellets and has certain strength, which is convenient to collect and transport. It is also convenient to use magnesium slag instead of limestone as a slagging agent in steel-making. However, all magnesium slag in its stock yard is in the form of powder. The powdery slag has a light bulk density and small particle size, and thus, it easily causes dust flying, polluting the environment and making recycling and use inconvenient. On the basis of research results on the stability of steel slag, the volume stabilization of magnesium slag can be achieved through two approaches: a physical method and a chemical method.

#### 4.1.2.1 Physical Stabilization of $C_2S$

The physical method to stabilize  $C_2S$  in magnesium slag is the rapid cooling of  $\beta$ - $C_2S$  via air cooling or water cooling to inhibit the transition into the  $\gamma$ - $C_2S$  phase and to prevent the formation of fine powder. Chan et al. prepared pure  $C_2S$  samples and then conducted a study on the stability of  $C_2S$  during the  $\beta \rightarrow \gamma$  phase transition under different cooling conditions [3]. They concluded that the inhibition of the phase transition from  $\beta$ - $C_2S$  to  $\gamma$ - $C_2S$  is related to the phase transition history, the driving force during cooling, and the amorphous phase of the dicalcium silicate sample. They also proposed a hypothesis regarding the critical particle size for the phase transition. Yang Qingxing et al. from Lulea<sup>a</sup> University of Science and Technology in Sweden conducted research on the physical method of stabilizing steel slag and effectively achieved the physical stabilization of steel slag under laboratory conditions [4, 5]. Jiang et al. of Anhui University of Technology studied aging changes of steel slag during a 20-day period after a rapid air cooling process [6]. Zhu of Nanjing Forestry University immersed steel slag in room-temperature water to reduce the volume expansion of steel slag and conducted a comparative experiment to study the strength of a steel slag mixture before and after the immersion treatment [7]. Professor Cui of Ningxia University conducted an experiment on the expansibility of magnesium slag and explored the expansion mechanism [8]. The author of this book also conducted air cooling and water cooling experiments on magnesium slag generated via the Pidgeon process and observed that the stabilizing effects of both cooling processes on the magnesium slag are obvious. Whether for steel slag or for magnesium slag, it is easy to stabilize  $C_2S$  through physical method under experimental conditions. However, on industrial production sites, energy consumption and site conditions must be considered, and it are normally difficult to meet the requirements of the continuous and stable treatment of large quantities of slags.

### 4.1.2.2 Chemical Stabilization of C<sub>2</sub>S

Chemical stabilization of C<sub>2</sub>S is accomplished by adding a small amount of chemical agents that contains certain ions to form a solid solution. The solid solution enters into C<sub>2</sub>S grains or is present at the grain boundaries, and this inhibits the phase transition from β-C<sub>2</sub>S to γ-C<sub>2</sub>S, thereby avoiding the powdering of magnesium slag caused by volume expansion; this reduces the damage that dust pollution causes to the environment. Kawasaki Iron and Steel Company of Japan used chemicals containing P<sub>2</sub>O<sub>5</sub> and B<sub>2</sub>O<sub>3</sub> to study the stability of stainless steel slag and found that following methods can be used to stabilize β-C<sub>2</sub>S: (1) The original Si<sup>4+</sup> or Ca<sup>2+</sup> ions are substituted with ions that have a radius smaller than that of Si<sup>4+</sup> or larger than that Ca<sup>2+</sup>. (2) Ions with a C/R (valence/ion radius) ratio < 2 or > 9.5 are used to substitute existing ions [2], as follows.

B <sup>3+</sup>	P <sup>5+</sup>	Si <sup>4+</sup>
0.22	0.33	< 0.4(Å)
Ba <sup>3+</sup>	Sr <sup>2+</sup>	Ca <sup>2+</sup>
1.36	> 1.16	> 0.99(Å)
1.36	> 1.16	> 0.99(Å)

In 2000 at the 6th international conference on molten slags, fluxes, and salts, German scientist Jürgen Geiseler introduced a series of elemental ions that can stabilize C<sub>2</sub>S, as shown in Fig. 4.2 [9].

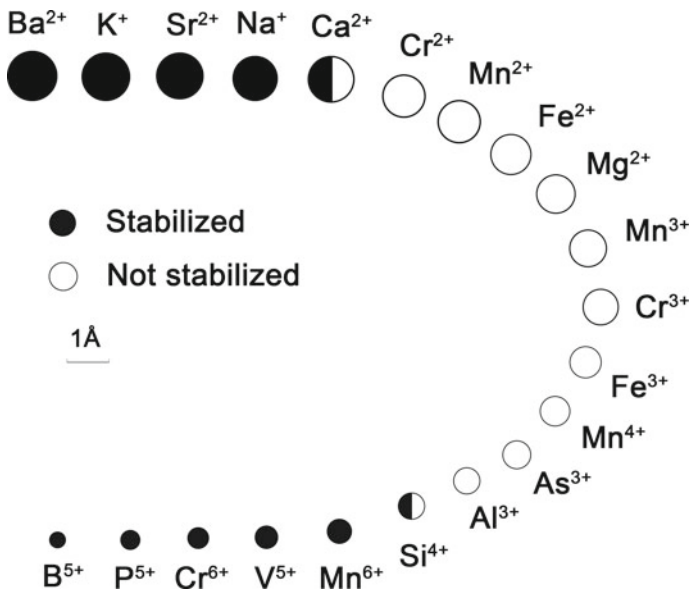


Fig. 4.2 Ions that can stabilize C<sub>2</sub>S

The author of this book added a mineralizer that contained P and B ions to magnesium slag. Experimental results confirmed that the added mineralizer stabilized magnesium slag. The experiments are described in detail in the following sections [10, 11]. Feng [12], Zhang [13], Huang [14], and other researchers have done similar research on steel slag and have drawn similar conclusions.

### 4.1.3 Experimental Study on Inhibition of $C_2S$ Phase Transition

This section introduces experimental research of the author's research group regarding the inhibiting of phase transitions of  $C_2S$  in magnesium slag, thereby reducing the degree of pulverization of magnesium slag.

#### 4.1.3.1 Phosphorus-Doping Experiment

To stabilize of  $C_2S$  in magnesium slag, make magnesium slag be lumpy and easy to collect, store, and transport. The lumpy magnesium slag diminishes the dust pollution caused by powdering of the slag and increases the proportion of  $\beta$ - $C_2S$  with gelling activity in the slag, which is favorable for using magnesium slag in construction materials [10]. Commercial phosphates were used as stabilizers for  $C_2S$ , and stabilization tests of magnesium slag were carried out.

**Experimental material:** The magnesium slag used in the experiments came from Fugu District Plant of Huiye Magnesium Group Co., Ltd. in Ningxia province. The main composition of the slag is shown in Table 4.1.

The phosphate stabilizers used in the experiment include fluorapatite, containing 17% phosphorus (industrial grade, Sihui Feilailfeng Non-metallic Mineral Material Co., Ltd.); calcium dihydrogen phosphate containing 22% phosphorus (food-grade, Lianyungang Xidu Biochemical Co., Ltd.); and calcium dihydrogen phosphate containing 22% phosphorus (feed-grade, Mianyang Shenlong Feed Co., Ltd.). Similar products produced in Sweden were tested for comparison. The added amount of stabilizer ranged from 0.5 to 8 wt%.

**Main equipment:** An X-ray diffractometer (Shimadzu XRD-6000), a laser particle size distribution analyzer (Honeywell Microtrac X-100), and an ultraviolet spectrophotometer (Beijing General TU-1810) were used.

**Experimental procedures:** Magnesium slag was placed in a vibrating mill and ground for 3 min; then, it was passed through a 40-mesh sieve, and kept for later use.

**Table 4.1** Composition of the magnesium slag sample used in the phosphorous experiment

Composition	MgO	CaO	SiO <sub>2</sub>	P <sub>2</sub> O <sub>5</sub>	Fe	Al	Mn	Na	CaO/SiO <sub>2</sub>
%	5.12	42.35	26.78	0.061	3.85	0.604	0.061	0.979	1.58

The three types of phosphate reagents were added separately to the magnesium slag and stirred well. The uniform mixture was poured into a steel mold of  $20 \times 20$  mm and pressed under 400 MPa using a hydraulic presser. After pressing, the samples were placed in a muffle furnace and calcined. The temperature was increased to 1200 °C and kept for 6 h. Then, the power was turned off, and the samples were subjected to furnace cooling. The phenomenon was observed after the samples were removed from the furnace. The amounts of stabilizer that were added to the slag were 1, 2.5, and 5% for the first group of samples and 0.5, 2, 4, and 8% for the second group of samples.

**Analysis of results:** (1) Morphology observation: The appearance of the first group of sintered samples is shown in Fig. 4.3a and that of the second group of samples is shown in Fig. 4.3b. In the figure, the blank sample is the reference magnesium slag sample without stabilizer. The reference samples were severely powdered; in contrast, all of the samples with stabilizers remained intact, and they are still not powdered after being stored for one month.

(2) XRD analysis: The XRD patterns of stabilized samples are shown for comparison in Fig. 4.4, where (a) is the reference sample without an added phosphorous compound, (b) is magnesium slag with 5 wt% of food-grade calcium dihydrogen phosphate, (c) is magnesium slag with 5% feed-grade calcium dihydrogen phosphate, and (d) is magnesium slag with 5% fluorapatite.

As seen in the XRD patterns, the diffraction peaks of the  $\gamma$ -C<sub>2</sub>S phase in the phosphorus-stabilized sample are reduced significantly compared to the diffraction peaks of the reference sample. The strong diffraction peaks near  $2\theta = 30^\circ$  disappear. The results indicate that in phosphorus-stabilized samples,  $\gamma$ -C<sub>2</sub>S decreased and  $\beta$ -C<sub>2</sub>S increased compared to the reference sample without stabilized agents. Also, the

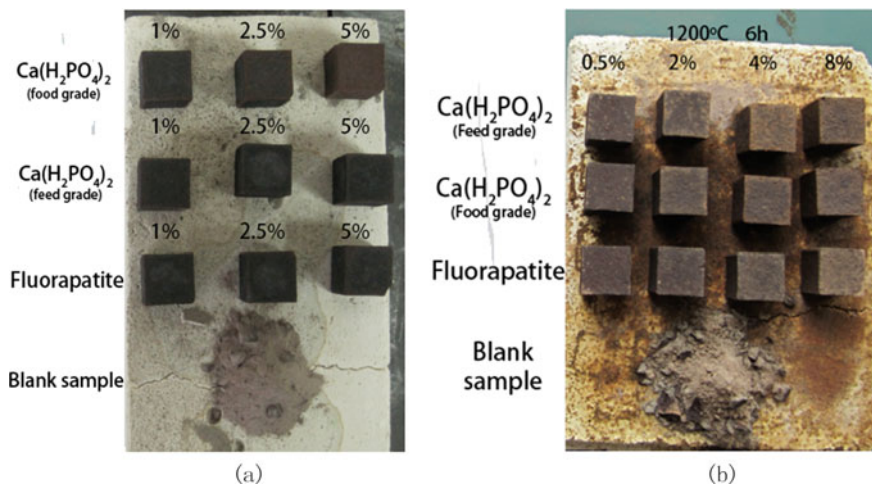


Fig. 4.3 Morphology of phosphorous-stabilized samples

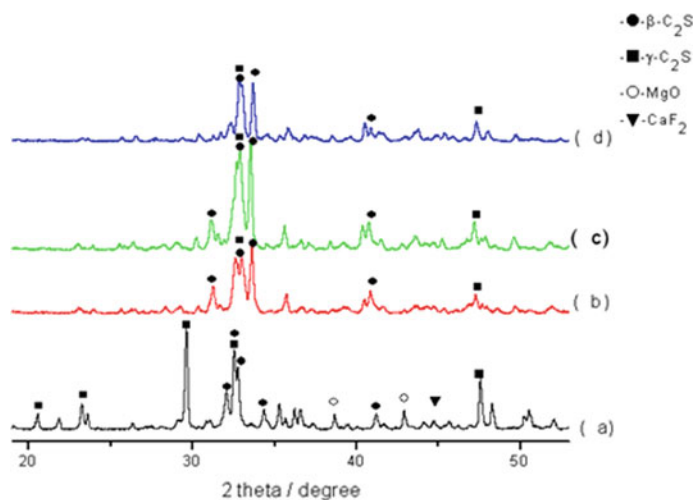


Fig. 4.4 XRD patterns of phosphorous-stabilized samples

three phosphorus-containing stabilizers do not show significant differences in the stabilizing effect.

Within a temperature range of 900–1200 °C, Fig. 4.5 shows the existential state of phosphorus simulated by Factage 6.2 using the compositions of the phosphorus-stabilized sample as the input data for the software. As seen from the figure, at high temperature, the added phosphorus acts in the form of a phosphate radical and forms a solid compound with calcium (or fluorine).

#### 4.1.3.2 Boron-Doping Experiment

Using boron-containing compounds as stabilizers to modify magnesium slag can suppress powdering and dusting of magnesium slag. This reduces the harm that magnesium slag can cause to the environment and improve the environmental conditions of a slag field and its surroundings [15, 16].

**Experimental materials:** The magnesium slag used in the experiment was from the Fugu Plant of Ningxia Huiye Magnesium Co., Ltd. Three types of borate reagents were used as stabilizers to investigate the effect that borate reagents have on preventing magnesium slag from powdering. Table 4.2 lists the compositions and melting points of three boron-containing compounds: anhydrous borax ( $B_4Na_2O_7$ ), G-VitriBore 25, and boric acid ( $H_3BO_3$ ). These three types of boron-containing compounds are all commercially available chemical reagents and are referred to as DB, GB, and H1, respectively. At higher temperature, the  $B_2O_3$  and  $Na_2O$  in DB and GB also have a certain stabilizing effect on polymorphic  $C_2S$ . These two boron-containing compounds are also reagents that are commonly used as dusting inhibitors of steel slag in many plants. Before use, all three of these boron-containing

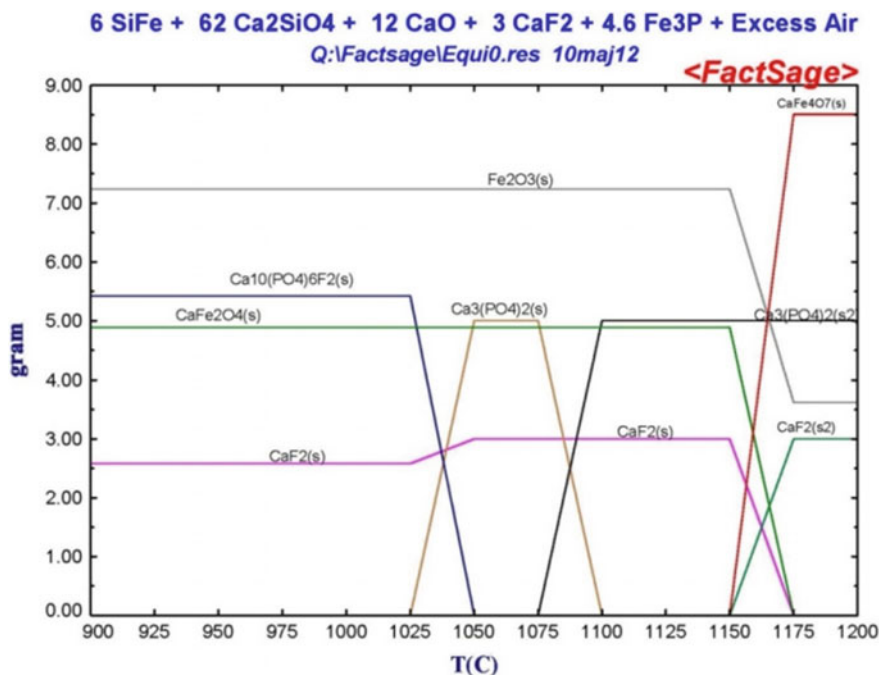


**Fig. 4.5** Behavior predictions of phosphorous-containing magnesium slag in the range of 900–1200°C

**Table 4.2** Contents (wt%) and melting points (°C) of boron-containing compounds

Borate	CaO	SiO <sub>2</sub>	B <sub>2</sub> O <sub>3</sub>	Na <sub>2</sub> O	MgO	P <sub>2</sub> O <sub>5</sub>	Melting point
DB			69	30.8			742
GB	8.8	29.4	23.5	23.5	0.3	1.4	696
H1			56.5				

compounds were ground and sieved as described above. Table 4.2 shows the main compositions and melting points of these boron-containing compounds.

### Preparation of samples

Magnesium slag must be dried before it is used; 30 mg of dried magnesium slag was mixed with each of the above three boron-containing compounds. The mass fraction of the added boron-containing compound was 0–1 wt% of the magnesium slag. A hydraulic presser was used to press the mixture into a square block with dimensions of 40 × 40 × 6 mm. The pressed compact blocks were placed in a muffle furnace, and the temperature was increased to 1200 °C. The samples were kept at this temperature for 2–6 h to carry out the sintering. The sintered blocks were then furnace-cooled. The samples were removed, and the cooled magnesium slag samples were examined to evaluate the effects of the boron-containing stabilizers.



### Morphologies and phases of samples

Figure 4.6 shows the morphology of the first group of samples, which were sintered at 1200 °C and held for 5 h. Among the samples, sample (a) is the reference sample without stabilizer, (b) is the sample with 0.53 wt% DB, and (c) is the sample with 0.54 wt% GB. Figure 4.7 shows the morphology of the second group of test samples, which were sintered at 1200 °C and held for 6 h. In Fig. 4.8, a is the magnesium slag with 0.59 wt% boric acid, (b) is the magnesium slag with 0.95 wt% boric acid, (c) is the magnesium slag sample with 0.34 wt% DB, and (d) is the reference sample without stabilizer. The results of the phosphorus-stabilized experiment are similar to those of the magnesium slag sample without stabilizer, which were severely powdered after cooling. Specifically, the test piece disintegrated and collapsed into fine powders. However, the sample with a boron-containing stabilizer basically retained the original morphology. A comparison of the different stabilizers indicates that the stabilizing effect of DB (anhydrous borax) is not as good as those of GB, G-Vitribore 25, and boric acid. In particular, in the second group of experiments, damage occurred in the sample with the DB stabilizer after a longer of holding time.

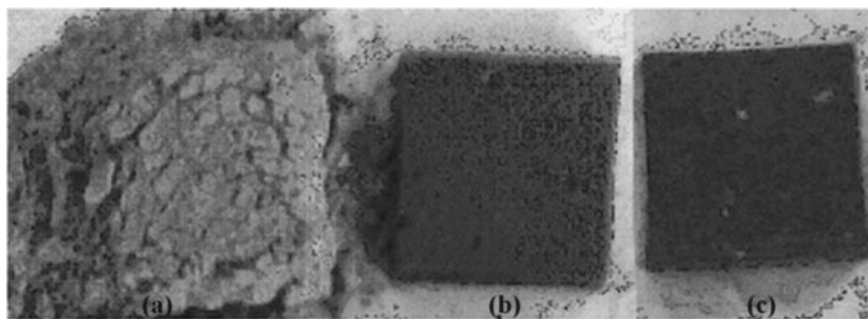


**Fig. 4.6** Morphologies of boron-stabilized slag samples in group 1: **a** reference sample without stabilizer, **b** sample with 0.53 wt% DB, and **c** sample with 0.54 wt% GB

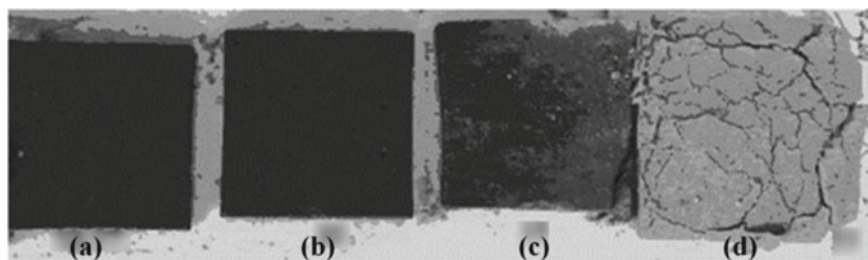


**Fig. 4.7** Morphologies of boron-stabilized slag samples in group 2: **a** sample with 0.59 wt% of boric acid, **b** sample with 0.95 wt% of boric acid, **c** sample with 0.34 wt% DB, and **d** reference sample without stabilizer

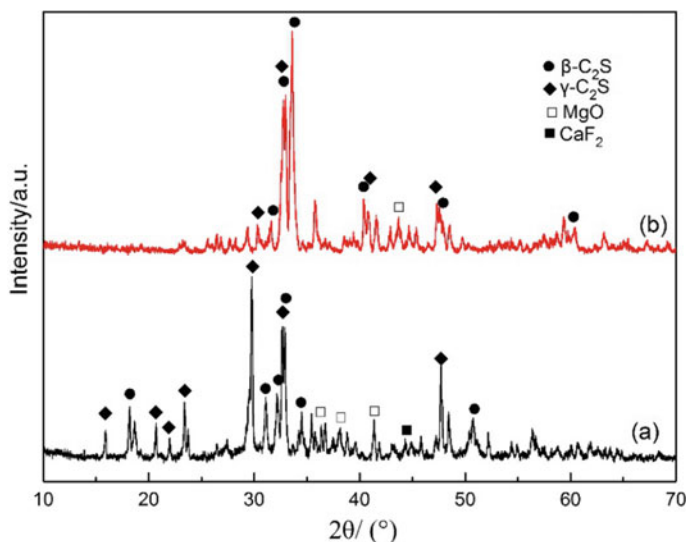


**Fig. 4.8** XRD patterns of boron-stabilized samples: **a** reference sample and **b** sample with 0.53 wt% DB

The phase analysis of the original magnesium slag, which served as a reference sample, and of the sintered magnesium slag with a boron-containing compound was carried out using an X-ray diffractometer (Shimadzu X-6000). The XRD patterns are shown in Fig. 4.8.

In Fig. 4.8, (a) is the reference sample without a stabilizer and (b) is the sintered magnesium slag sample with 0.53 wt% DB. As seen from the XRD pattern of the reference sample in Fig. 4.8a,  $\gamma$ - $C_2S$  is the main phase, and it is the main reason that the powdering phenomenon of magnesium slag occurs.  $\beta$ - $C_2S$  is detected as a secondary phase, and this indicates that a small amount of  $\beta$ - $C_2S$  is present in the powdered magnesium slag. Magnesium oxide is also present. A trace amount of  $CaF_2$  is also detected, and it only accounts for 2.5–3 wt% in the raw materials. As seen in Fig. 4.8b, the content of  $\gamma$ - $C_2S$  in the magnesium slag sample with 0.53 wt% DB after sintering was significantly lower than that in the reference sample. Also,  $C_2S$  was mainly present in the form of the  $\beta$ - $C_2S$  phase, indicating that the added boron ions inhibited the phase transition from  $\beta$ - $C_2S$  to  $\gamma$ - $C_2S$  in the sample. Interestingly, the diffraction peaks of MgO were also weakened, and this is possibly because some of the free MgO in the slag was stabilized in the stationary phase. The  $CaF_2$  phase was not detected.

The results of the boron-stabilized samples are similar to those of the phosphorus-stabilized samples. Compared with the reference sample, the diffraction peaks of the  $\gamma$ - $C_2S$  phase in the boron-stabilized sample were significantly reduced; the strongest  $\gamma$ - $C_2S$  diffraction peak at a  $2\theta$  angle near  $30^\circ$  was much weaker, and the intensity was significantly lower.

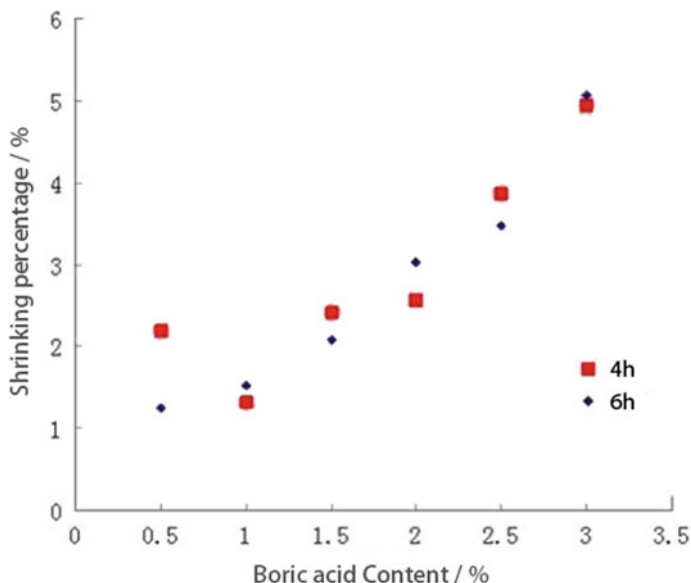


Fig. 4.9 Shrinkage rates of samples with added amounts of borate acid

### Shrinkage and influencing factors

The volume shrinkage of samples with different contents of boric acid was measured after sintering. The volume shrinkage rate is equal to the value of (volume of original sample minus volume of sintered sample)/volume of original sample. The changes in shrinkage with respect to mineralizer content are shown in Fig. 4.9. The data represented by red squares in the figure are the shrinkage of the sample after 4 h of temperature holding time, and the data represented by black diamonds are the shrinkage of the sample after 6 h of temperature holding time.

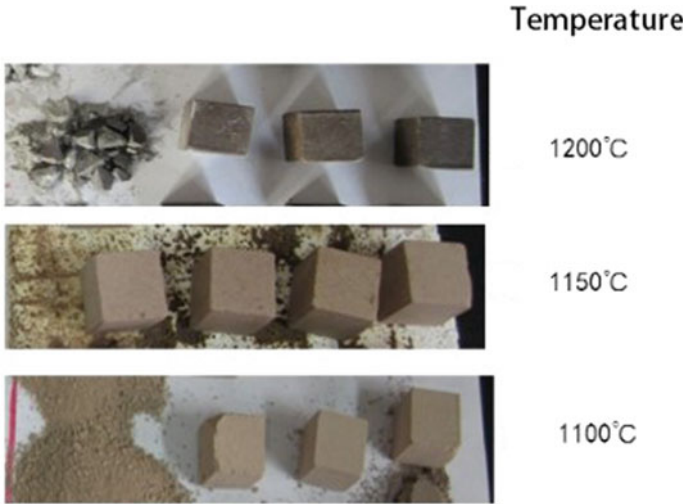
As seen in Fig. 4.9, the overall shrinkage of the sintered samples increase linearly with an increase in the amount of added boric acid. There are no essential differences between the results for the samples that had temperature holding times of 4 and 6 h. In particular, the shrinkage of samples with different temperature holding times is almost consistent when the amount of added boric acid reached a maximum value of 3%.

#### 4.1.3.3 Doping Experiment Using Rare Earth Oxides

In the doping experiment, the rare earth oxides  $\text{La}_2\text{O}_3$ ,  $\text{Y}_2\text{O}_3$ , and  $\text{Ce}_2\text{O}_3$  (purchased from Baotou Rare Earth Research Institute) were used as stabilizers. The percent range of the added rare earth oxide stabilizer was 0.5–5%. The experimental temperatures were 1100, 1150, and 1200 °C, and the holding time range was 0.5–6 h. The other experimental conditions were the same as those in previous phosphorus-doping

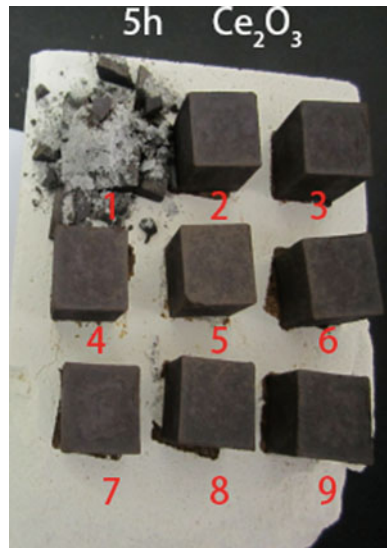
and boron-doping stabilization experiments. Figures 4.10, 4.11 and 4.12 show photos from  $Ce_2O_3$ -doping (or  $La_2O_3$ -doping) stabilization experiments.

Figure 4.10 shows photos of samples with  $Ce_2O_3$  used as a stabilizer. The sample was held at temperatures of 1200, 1150, and 1100 °C for 6 h, and the amount of added stabilizer gradually increased (0.5–5%) in the samples that are shown from left to right. As seen in the figure, a large percentage of stabilizer is beneficial for volume

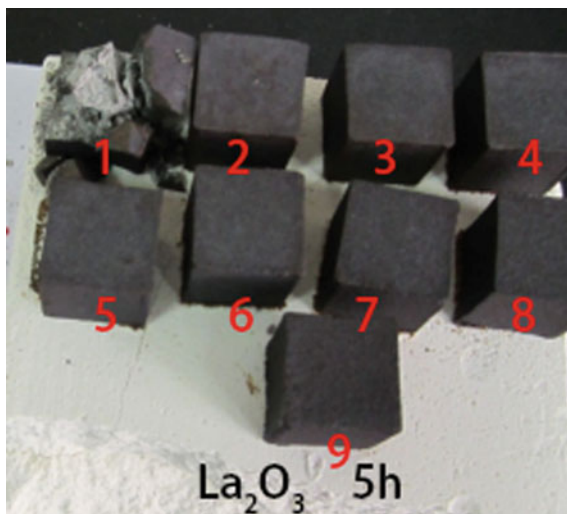


**Fig. 4.10** Stabilizing effects of  $Ce_2O_3$ -doping at different temperatures

**Fig. 4.11** Stabilizing effects of  $Ce_2O_3$ -doping



**Fig. 4.12** Experimental effects of the  $\text{La}_2\text{O}_3$  doping experiment



stability of magnesium slag; the sample that was held at a temperature of 1200 °C had the best compactness and the largest volume shrinkage. For comparison, Fig. 4.11 shows photos of samples that had different amounts of added  $\text{CeO}_2$  with a holding time of 5 h and a temperature of 1200 °C. Compared to the results of samples that had a holding time of 6 h, there are no significant differences. As seen from several sets of experimental photos, the sample with the minimum added amount of 0.5% obviously did not meet the requirements for stabilizing magnesium slag.

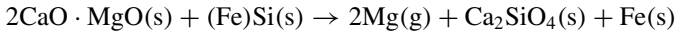
Figure 4.12 shows photos of samples that used  $\text{La}_2\text{O}_3$  as a stabilizer. The samples were held at 1200 °C for 5 h, and the amount of added  $\text{La}_2\text{O}_3$  increased continuously in the samples ordered #1–#9, which had increasing content from 0.5–3 wt%. It is clear from Fig. 4.12 that  $\text{La}_2\text{O}_3$  has a remarkable stabilizing effect. However, because of the costs of practical applications, the role that rare earth oxides play in stabilizing magnesium slag has not been further studied

## 4.2 Reduction of Fluorine in Magnesium Slag

### 4.2.1 Catalytic Effects of Calcium Fluoride on Reduction of Mg

The traditional silicothermic process of magnesium smelting via Pidgeon process is to reduce dolomite using ferrosilicon at 1200 °C under negative pressure. Calcium fluoride acts as a catalyst in the silicothermic reduction and does not participate in the reaction. Therefore, after the reaction is complete, most of the fluorine-containing components remain in the slag.

The chemical reaction of smelting magnesium via the Pidgeon process is as follows:



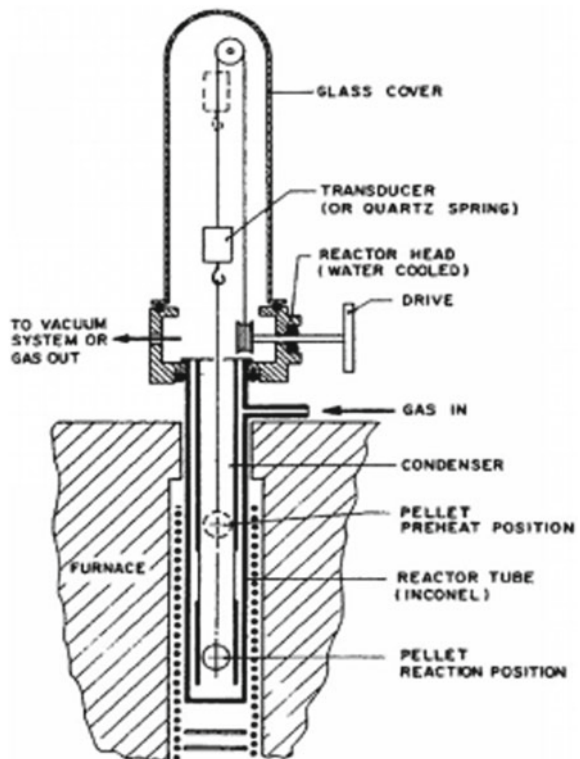
The main raw materials that are used in magnesium smelting include calcined dolomite ( $\text{CaO} \cdot \text{MgO}$ ), ferrosilicon  $(\text{Fe})\text{Si}$ , and fluorite ( $\text{CaF}_2$ ). In industry, the proportion of raw materials is usually as follows:

calcined dolomite: ferrosilicon: fluorite = 100:20:3

The converted mass ratio is as follows: 81.3:16.3:2.44 (wt%)

Barua et al. [17] used the simulated experimental device shown in Fig. 4.13, prepared a pellet of magnesium smelting raw material, and hung it on a quartz wire to detect the weight loss of the pellet during the reaction. The temperature inside the reactor was controlled to be between 1070-1250 °C.  $\text{H}_2$  gas was introduced into the reactor with a flow rate of 6 l/min, so that the Mg vapor that is generated via the reduction reaction can leave the reactor with  $\text{H}_2$  gas when a flow of  $\text{H}_2$  gas is passed through the pellets. As a result, the Mg vapor pressure on the surface of the pellet is close to the pressure of vacuum magnesium smelting, and this meets the

**Fig. 4.13** Equipment used in the kinetically simulated magnesium smelting experiment (Reprinted from Ref. [17] Copyright 1981, with permission from Taylor & Francis Group)



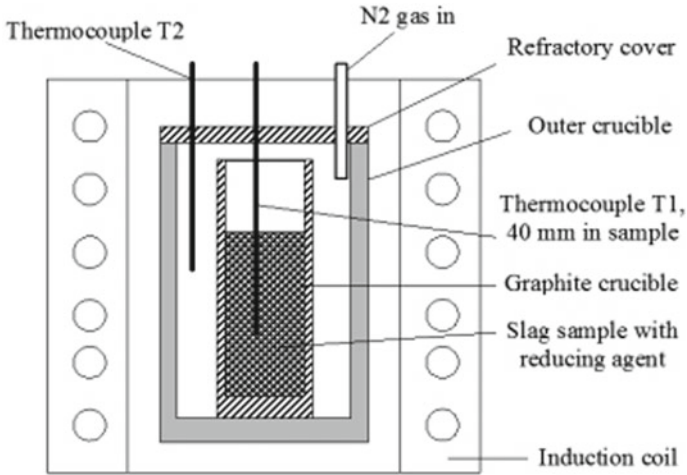


**Fig. 4.14** Reduction experiment equipment used in smelting magnesium

thermodynamic conditions of vacuum magnesium smelting. In addition to measuring the weight loss of the pellet in the test, Barua et al. also analyzed and characterized the pellet after the test. They used theoretical calculations and obtained research results on the kinetics conditions for magnesium smelting. The author of this book used a device, as shown in Fig. 4.14, to carry out silicothermic reduction of  $\text{MgO}$  using  $\text{CaF}_2$  as a catalyst. In the magnesium smelting simulation experiment, a nozzle was used to blow  $\text{N}_2$  directly into a small crucible to reduce the partial pressure of magnesium vapor on the surface of the raw material in magnesium smelting. As shown in the figure, the thermocouple T1 was buried in the center part of the experimental sample to measure the temperature inside the sample. The thermocouple T2 was fixed in the furnace cavity to measure the furnace temperature.

Figure 4.15 shows the curves of the sample temperature and furnace temperature that were measured with respect to time under experimental conditions. The experimental raw material had a weight of 350 g, and the proportion was according to the industrial standard (including fluorite) for magnesium smelting. The temperature inside the sample ( $T_1$ ) is marked in red, and the temperature inside the furnace ( $T_2$ ) is marked in blue. As seen in Fig. 4.16, during the first 50 min of the simulation experiment,  $T_1$  was always lower than  $T_2$ .  $T_1$  began to increase rapidly after 45 min, caught up with  $T_2$  at about 50 min and remains close to  $T_2$  until the end of the experiment. To study the effect that the mineralizer has on the temperature inside the material used in the simulated magnesium smelting experiment, the rate of temperature increase inside the material (i.e., the heating rate) was calculated using the following Formula:

$$\text{Heating rate} = \Delta T / \Delta t$$

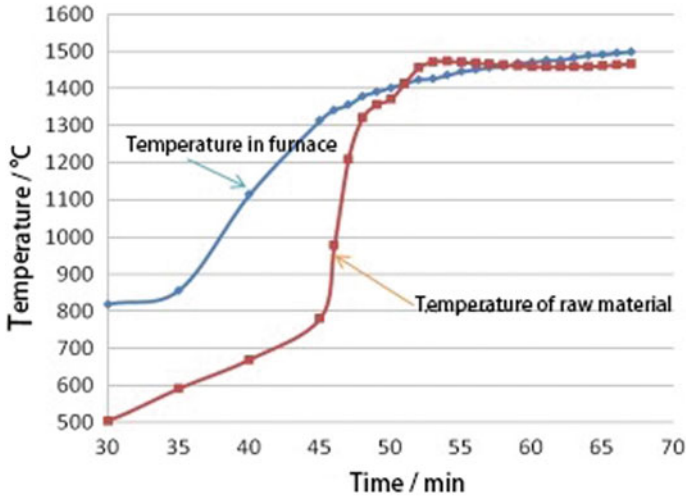


Fig. 4.15 Changes in temperature inside the material (T1) and inside the furnace (T2) with respect to time

where  $\Delta T$  denotes the temperature difference between two adjacent points of measurement, and  $\Delta t$  is the time interval of the temperature measurement.

For the simulation tests with and without  $\text{CaF}_2$ , the changes in the material's heating rate relative to the furnace temperature are shown in Fig. 4.16. In the

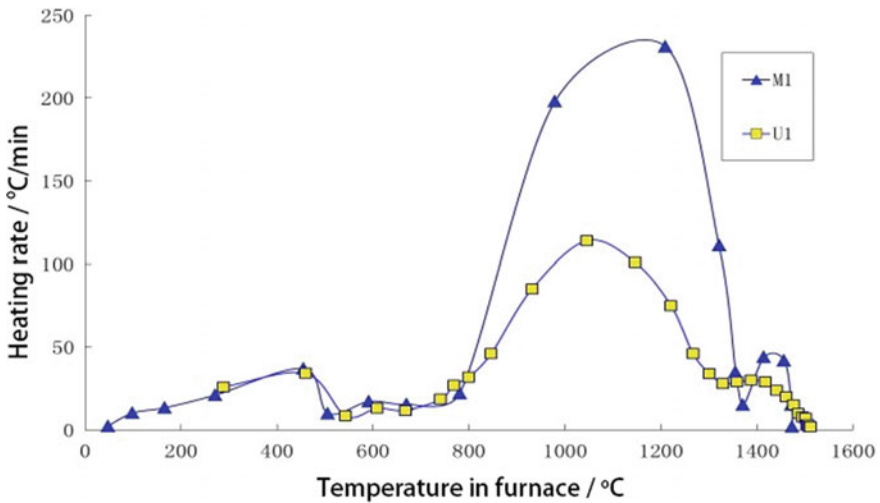


Fig. 4.16 Effects of  $\text{CaF}_2$  on the heating rate of raw materials in magnesium smelting



figure, M1 is a standard formulation of material for magnesium smelting production containing calcium fluoride, and U1 has the same formulation as M1 but does not contain calcium fluoride.

In the low temperature stage (below 800 °C), the heating rates of the two test materials are similar. Starting from a furnace temperature above 800 °C, the heating rate of M1 observably increases, and it is close to 250 °C/min at a furnace temperature of 1200 °C. The heating rates of the raw materials are closely related to the reaction rate of magnesium smelting. As ferrosilicon melts at high temperature, a liquid phase is generated, and the flow of the liquid phase greatly improves the kinetics conditions of the reduction reaction, accelerating the reaction. Therefore, the heating rates of samples with and without CaF<sub>2</sub> both start to increase. However, the comparison between M1 and U1 curves clearly show that the heating rate of M1 containing CaF<sub>2</sub> is almost double that of U1 without CaF<sub>2</sub>; this indicates that adding CaF<sub>2</sub> increases the heating rate significantly, thereby increasing the reduction rate of MgO. The experimental results confirm that the catalytic effect of CaF<sub>2</sub> as a mineralizer is very obvious in the reduction of magnesium oxide.

## 4.2.2 Magnesium Smelting Pilot Test

### 4.2.2.1 Equipment Used in the Pilot Test

To be as close as possible to the actual production conditions of magnesium smelting via the Pidgeon process and to optimize the formula of the raw materials, a pilot test was used to simulate magnesium smelting experiments. The reduction retort used in industry was scaled down, and two identical retorts that can each hold 10 kg of raw materials were designed and manufactured. The reduction retorts were placed side-by-side in a muffle furnace with temperature control. The furnace size of the muffle furnace was 810 × 550 × 375 mm; the equipment power was 25 kw, and the heating rate was controllable. It takes about 2.5–3 h for the furnace to reach 1130 °C. Two-stage vacuum pumps were connected in series to ensure that the vacuum in the reduction retort reached 7–13 Pa, and this meets the requirements for magnesium smelting. The reduction retort was made of heat-resistant steel pipe. One end of the pipe was sealed, and other end was welded with a water-cooling jacket. To simulate industrial production conditions, an experimental device was established to compare materials with the standard formula of the Pidgeon process and the experimental formula. A schematic diagram and actual photos of the pilot experimental system are shown in Fig. 4.17. A schematic diagram of the structure of the reduction retort is shown in Fig. 4.18.

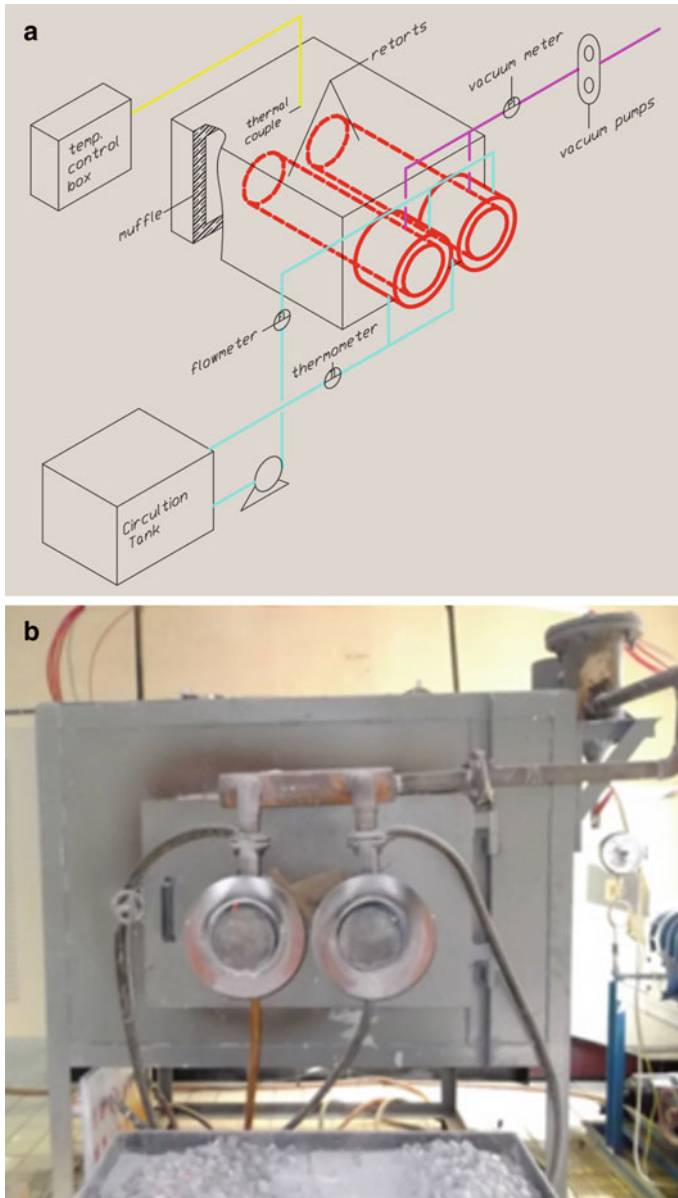
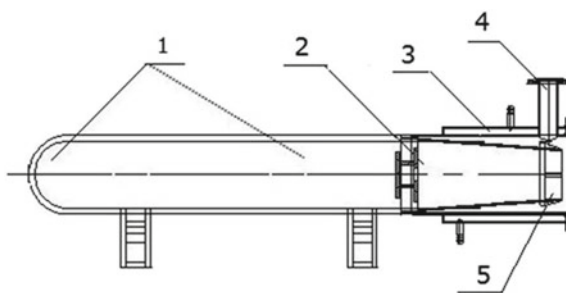


**Fig. 4.17** Experimental equipment used to simulate magnesium smelting via the Pidgeon process **a** schematic diagram of the equipment's system and **b** photo of experimental equipment

**Fig. 4.18** Schematic diagram of reduction retort in pilot magnesium smelting equipment 1—reduction retort 2—Mg Crystallizer 3—water jacket 4—vacuum interface 5—K/Na Crystallizer



#### 4.2.2.2 Process Flow of Pilot Magnesium Smelting Test

The pilot-scale magnesium smelting process imitates the production process of metallic magnesium, as shown in Fig. 4.19. The raw materials that were used in the simulated experiment included calcined dolomite, fluorite, and ferrosilicon, which were all obtained from Ningxia Huiye Magnesium Group Co., Ltd. The raw materials were crushed to pass through 100 mesh, mixed with different mineralizers,

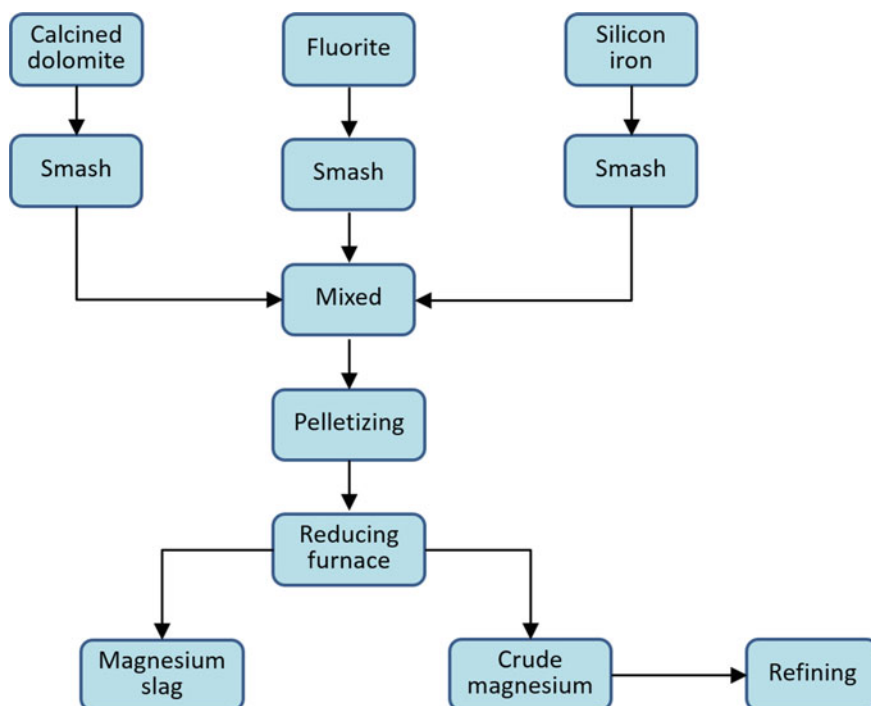


**Fig. 4.19** Process flow of pilot magnesium smelting test

compressed into blocks with similar volume as the production pellets, packed into a paper bag, and placed into the retort of the pilot furnace for a comparison experiment.

The magnesium smelting process used in the experimental furnace is as follows: In the first stage, the furnace temperature was increased to 1150 °C, and then the compressed blocks of material were placed in the reduction retorts. The sample with the standard formula used in magnesium smelting production was placed in the left reduction retort (A) as the reference sample, and the sample with the experimental formula was placed in the right reduction retort (B). After the loading was complete, the mouths of the retorts were closed, and the first-stage vacuum pump was started. When the vacuum reached 80 Pa, the second-stage vacuum pump was started and run until the vacuum reached 7–13 Pa. (See the production parameters of magnesium smelting.) The current was 65 A, and the flow rate of the water in the cooling jacket was 15–20 L/h. After the reaction was complete, the power was cut off, and the furnace was cooled. Finally, the vacuum pump was turned off; the furnace mouth was opened, and the magnesium crystallizer was removed. The magnesium slag was removed and cooled to room temperature. The magnesium slag was sieved using a 40-mesh standard sieve, and then the oversize rate of the magnesium slag was calculated. The range of the reduction temperature during the entire smelting process was 1195–1205 °C, and the reduction cycle was 400 min. The inner layer of the reduction retort wall was made of heat-resistant steel and might desquamate under high temperature and oxidation conditions; small pieces of iron scraps enter the magnesium slag and may affect the accuracy of the calculated weight composition of magnesium slag.

#### 4.2.2.3 Influence of the Pellet Formation Method on Magnesium Smelting

To ensure the complete reaction of raw materials in the reduction retort, the raw materials must be pressed into briquette-sized pellets with certain strength. If the pellets are not strong enough, they break easily during the filling and reaction process and affect the reaction. However, pellets that are too dense are not conducive to the escape of magnesium vapor, which is also inadvisable. Industrial production requires a special pelletizer to prepare pellets of the raw materials. Because many varieties and small quantity of materials were used in the experiment, steel molds were used to press the sample block. To verify the influence that the formation method has on the yield of crude magnesium, one reduction retort was filled with the pellets that were made in the factory pelletizer, whereas the other reduction retort was filled with sample blocks that had the same weight and composition and were pressed in the laboratory press. They were smelted at the same time in the pilot furnace. The respective crude magnesium yields were compared, and the results are shown in Table 4.3.

The following observations are made from Table 4.3: (1) The vacuum, cooling, and heating systems of the pilot system are normal during the blank sintering experiment. Blank sintering was carried out 10 times. (2) The contents of the left and right retorts are consistent, and the magnesium yields are almost the same; this indicates that the

**Table 4.3** Comparison experiment of the sample formation method

Number of experiment	Raw materials	Crude magnesium output/kg		Note
		Left retort	Right retort	
1				Blank experiment with normal running
2	Each retort has 10 kg of raw material pellets	1.65	1.65	The materials in both retorts have the same formula. All samples were pressed and shaped by a pellet-presser of industry
3		1.85	1.85	
4		1.65	1.65	
5		1.85	1.85	
6		2.00	2.05	
7	right retort: 10 kg of pellets from magnesium plant; left retort: 10 kg of pressed blocks	1.20	1.30	The materials in the left and right retort have the same formula; the sample in the right retort is formed by a pellet-presser of industry, and the sample in the left retort is shaped in Lab
8		0.75	1.40	
9		1.45	1.45	
10		1.60	1.70	
11		1.70	1.80	

reaction consistency between the left and right retort is remarkable. (3) The left and right tanks were respectively loaded with pellets made in a magnesium plant and with laboratory-pressed blocks. When the raw material formulations were identical, the crude magnesium yield of laboratory-pressed blocks was slightly lower than that of factory pellets (the result of the 8th group was abnormal), and the error was less than 10%. The formation method of the experimental sample blocks can be used to simulate the industrial pellet formation method for raw materials used in industrialized magnesium smelting.

### 4.2.3 Migration of Fluorine in Magnesium Smelting

In magnesium smelting via silicothermic reduction, it is necessary to add about 3 wt% of fluorite (containing 95 wt% calcium fluoride,  $\text{CaF}_2$ ) as a mineralizer of magnesium reduction. The fluorine in calcium fluoride does not react with magnesium and only serves to promote the reaction. After the reaction is complete,  $\text{CaF}_2$  is discharged with

magnesium slag. Feng et al. [18] once believed that fluorine became gaseous under the high temperature in magnesium smelting and that the gaseous fluorine was pumped out using vacuum system, escaping into the atmosphere. To verify the whereabouts of fluorine, the author's team used the pilot test equipment for magnesium smelting to investigate Gao's statement, and the results are discussed [19]. The experimental data are shown in Tables 4.4 and 4.5. The fluorine balance in Table 4.5 was calculated using the experimental data in Table 4.4.

As seen from the fluorine balance shown in Table 4.5, after the reaction was complete, most of the fluorine added to the silicothermic reaction system with raw materials can be detected in the magnesium slag. This may occur because of the following reasons:  $\text{CaF}_2$  in the raw material pellets decomposes into gas at a temperature above  $1000\text{ }^\circ\text{C}$  in the front zone of the reduction retort and moves to the rear zone of the reduction retort under the driving of vacuum power. When it reaches the rear cooling zone using circulating water, it condenses into a solid as the temperature drops. Because fluorine does not participate in the reaction, it is finally discharged with the magnesium slag. Therefore, most of the fluorine is not discharged directly via the vacuum system, but it is present in magnesium slag in the form of solid fluorine-containing compounds.

Figure 4.20 shows the relationship between the calculated value of fluorine in the raw material pellets and the measured fluorine content in the magnesium slag samples. As seen from the figure, the fluorine content in magnesium slag is directly proportional to the fluorine content in the raw material.

FactSage<sup>TM</sup> (FactSage 6.2) was used to simulate and calculate the migration and change of fluorine during the magnesium smelting process [19]. Table 4.6 lists the initial formulation of the input raw materials using in the simulation calculation. (The total amount was 100 g.) The proportion of each material component refers to that in the magnesium smelted via the Pidgeon process. The temperature range was  $100\text{--}1200\text{ }^\circ\text{C}$ , and the pressure was 10 Pa. Figure 4.21 shows a schematic diagram of changes in components with respect to temperature changes in the FACTSAGE-simulated magnesium smelting process; as seen, some components disappear and new phases form.

On the basis of the above experimental results of simulated magnesium smelting, it can be inferred that the reduction slag of magnesium produced in the Pidgeon process contains most of the fluorine that was in the raw material fluorite. This part of fluorine is discharged with the reduction slag.

#### ***4.2.4 Influence of Fluorine on Reuse of Mg Slag***

In 2009, magnesium slag was included into national standard as a mixed material that can be used as cement production raw material. Magnesium slag contains a large amount of the silicate mineral  $\text{C}_2\text{S}$ . In addition to replacing some of the mineral raw materials when sintering cement clinker together with other raw materials,  $\text{C}_2\text{S}$  can serve as a crystal seed during the calcination process of cement materials to

**Table 4.4** Trace of fluorine in the smelting process

Expe. No.	Raw materials/kg			Products/kg			Fluorine in products/wt%		
	Calcined dolomite	Ferrosilicon	Fluorite	Mg slag	Crude Mg ingot	K/Na crystals	Mg slag	Crude Mg ingot	K/Na crystals
1	5.0	0.84	0.25	4.1	0.9	0.031	2.6	0.064	0.169
2	4.5	0.84	0.25	4.2	0.8	0.023	2.95	0.042	0.166
3	8.13	1.67	0.25	7.1	1.8	–	1.57	0.022	–
4	8.13	1.67	0.25	8.3	1.85	0.061	1.24	0.047	0.07

**Table 4.5** Fluorine balance

Number of experiments		1	2	3	4
Fluorine <sub>in</sub> /g	Raw materials	115.7	115.7	115.7	115.7
Fluorine <sub>out</sub> /g	Mg slag	106.6	123.9*	111.5	102.9
	Crude Mg ingot	0.58	0.34	0.4	0.87
	K/Na crystals	0.05	0.04	–	0.04
	total	107.2	124.3	111.9	103.8
Fluorine <sub>in</sub> –Fluorine <sub>out</sub> /g		8.5	–	3.8	11.9
Fluorine <sub>out</sub> /Fluorine <sub>in</sub> /%		92.68	–	96.69	89.74
Fluorine <sub>out</sub> / in Mg slag/%/Fluorine <sub>in</sub>		92.13	–	96.34	88.95

\*Note Measurement error may cause the results of experiment 2 for fluorine in magnesium slag to be larger than the amount of input fluorine

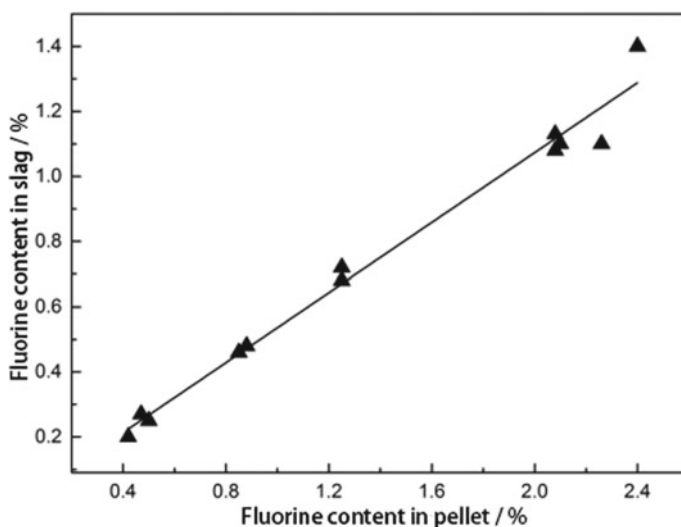


**Fig. 4.20** Relationship between the percent of fluorine in the raw materials and that in the corresponding magnesium slag

**Table 4.6** Input values of reactants in simulation calculations

Reactant	Si	Fe		CaO	MgO	CaF <sub>2</sub>	Na <sub>2</sub> O
Mass/g	12	4		56.1	25.2	2.5	1



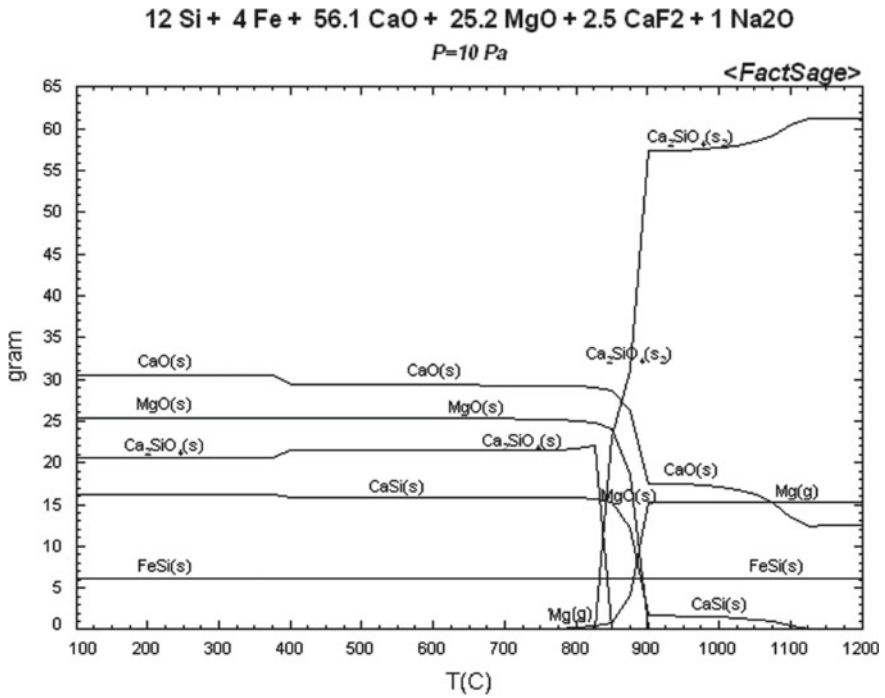


**Fig. 4.21** Changes in materials versus temperature in the simulated magnesium smelting process

reduce the potential energy in crystal nucleation. Thus, magnesium slag can be used to accelerate the formation of C<sub>3</sub>S and to promote the sintering of cement clinker. The CaO and SiO<sub>2</sub> that is contained in the magnesium slag can reduce the amounts of limestone and clay that are used in the raw materials of cement. This reduces the damage to the natural ecology that is caused by the excavation of the raw materials used in cement; it also reduces the energy consumption in processes during clinker calcination, such as clay dehydration and CaCO<sub>3</sub> decomposition. Therefore, using magnesium slag to prepare cement clinker has advantages that other metallurgical slags do not possess. However, under the high temperature of the sintering process of cement clinker, the CaF<sub>2</sub> in the magnesium slag becomes gaseous and volatilizes into the atmosphere. This therefore causes secondary pollution, which causes sufficient concern. For reuses of magnesium slag that require a high-temperature treatment, serious attention must be paid to the problem of fluorine evaporation.

Magnesium slag can replace limestone as the slagging agent used in steel-making. The results of the industrial test carried out at the Ningxia Steel Plant confirm that replacing 30% of limestone with magnesium slag as the slagging agent for steel-making was successful. However, the F components in magnesium slag might enter the molten steel, and this affects the quality of fluorine-free steel products. This requires further investigation and verification and cannot be easily ignored.

When magnesium slag is recycled and used, attention should be paid to the leaching of fluoride. The maximum fluorine emission in the National Standard of China GB5749-2006 for drinking water quality and safety is 10 mg/kg, and the leaching result of fluorine in magnesium slag far exceeds the permitted limit. If waste water is discharged during the treatment of magnesium slag, it can easily cause fluoride leaching and then pose a threat to the environment so researchers should pay special concern to it.

#### 4.2.5 Magnesium Smelting Using Fluorine-Free Mineralizer

To solve the problems of dusting and fluorine pollution of magnesium slag, a magnesium smelting pilot test was carried out using fluorine-free mineralizer instead of  $\text{CaF}_2$ . The test is divided into two parts: (1) using boron-containing compounds to replace  $\text{CaF}_2$  in magnesium smelting and (2) using rare earth oxides to replace  $\text{CaF}_2$  in magnesium smelting.

**Experimental materials:** The experimental materials used in the pilot test were from Ningxia Huiye Magnesium Group Co., Ltd. The main raw materials were calcined dolomite, ferrosilicon, fluorite, boron-containing compounds, and rare earth oxides. The mass fraction of  $\text{MgO}$  in dolomite is 31%, the mass fraction of silicon in ferrosilicon is 75%, and the mass fraction of  $\text{CaF}_2$  in fluorite is 95%. Industrial-grade boric acid ( $\text{H}_3\text{BO}_3 \geq 99.6\%$ ; sulfate  $\leq 0.08\%$ ) was selected as the boron-containing mineralizer, according to the results of the stability experiment. The rare earth oxides that were used in the experiments were cerium oxide ( $\text{CeO}_2$ ), lanthanum oxide ( $\text{La}_2\text{O}_3$ ), yttrium oxide ( $\text{Y}_2\text{O}_3$ ), and terbium oxide ( $\text{Tb}_2\text{O}_3$ ); all of rare earth oxides were purchased from Baotou Rare Earth Research Institute.

**Experimental equipment:** The pilot experimental equipment introduced in 4.2.2.1 was used. The sample in retort A of two parallel reduction retorts was the reference sample, the magnesium smelting raw materials were in accordance with the production formula, and fluorite was used as a mineralizer. The sample in retort B was the experimental sample, boron-containing mineralizers were used to replace some or all of the fluorite, and the other raw materials were consistent with the reference sample. The two retorts were placed under the same experimental conditions; specifically, the heating rate, magnesium smelting temperature, and degree of vacuum were completely identical.

**Experiment I** using a boron-containing compound to replace fluorite in magnesium smelting. Boric acid was selected as a typical boron-containing compound for the experiment. The experiment was divided into two parts: in experiment (a), all of the fluorite was replaced with boric acid, and in experiment (b), some of the fluorite was replaced with boric acid. In experiment 1(a), 8.13 kg dolomite and 1.67 kg ferrosilicon were added to each reduction retort. The amount of fluorite added to the reference group was 0.25 kg. No fluorite was added to the experimental group, and only different amounts of boric acid were added. The relationship between the amount of added boric acid and the yield of crude magnesium is shown in Fig. 4.22. The

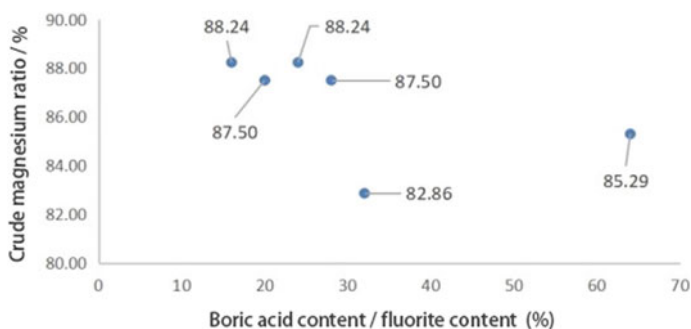


**Fig. 4.22** Influences that using  $H_3BO_3$  to replace fluorite has on the yield of crude Mg

abscissa in the figure is the percent of boric acid that was added to the experimental group with respect to the amount of fluorite in the reference group.

Crude magnesium ratio = yield of crude magnesium in experimental group/yield of that in reference group

As seen in Fig. 4.22, completely replacing fluorite with boric acid failed to achieve the yield of fluorite mineralizer. When the amount of added boric acid was 40–70 g (the amount of added boric acid/that of fluorite added in the reference group is 16–28%), the yield of crude magnesium fluctuates around 87–88%. With a further increase in the amount of boric acid, the yield of crude magnesium decreased inversely. When the amount of added boric acid reached the maximum value of 160 g (boric acid/fluorite is 64%), the crude magnesium yield was only about 85%. For the reference group, the crude magnesium output that obtained via magnesium smelting with fluorite was higher than that of the group in which boric acid was used as a mineralizer. To prevent boric acid from affecting the quality of crude magnesium that was produced via magnesium smelting, an X-ray diffractometer was used to perform elemental analysis on all crude magnesium products that were obtained in the experiments, and a high precision fluorimeter (fluoride ion selective electrode) was used to detect the fluorine content of samples. The test results confirm that the quality of the experimental crude magnesium samples was good and meets the standards for magnesium smelting products.

In experiment 1 (b), the two reduction retorts were loaded with same amounts of dolomite and ferrosilicon. To facilitate the experiment, the amounts of raw materials were reduced and the proportions of the raw materials remained unchanged. The sample in the reference group still followed the production formula and used fluorite as a mineralizer. The difference from experiment 1 (a) is that in experimental 1 (b), both fluorite and boric acid were added to reduce the amount of fluorite, which reduces fluorine pollution. The experimental data is shown in Table 4.7.

As clearly seen from the data in Table 4.7, the magnesium smelting experiment that used boric acid to partly replace fluorite achieved remarkable results. Under the same conditions, the crude magnesium outputs of most experimental groups were equal to or greater than that of the reference group that used fluorite as a mineralizer.

**Table 4.7** Experimental data of magnesium smelting with boric acid used to replace some of the fluorite

Experimental series		Proportion of mineral in raw materials/%			Oversize rate of Mg slag/%	Crude Mg ratio/%
		Fluorite	Boric acid	Total		
B1	Reference group	2.1	0	2.1	44	
	Experimental group	0.85	0.42	1.27	76	100
B2	Reference group	2.13	0	2.13	60	
	Experimental group	0.86	0.69	1.55	92	87.5
B3	Reference group	2.1	0	2.1	80	
	Experimental group	0.43	0.39	0.82	92	100
B4	Reference group	2.4	0	2.4	60	
	Experimental group	0.49	0.24	0.73	76	108
B5	Reference group	2.49	0	2.49	28	
	Experimental group	0.51	0.25	0.76	88	116.7
B6	Reference group	2.46	0	2.46	52	
	Experimental group	0.5	0.21	0.71	89	100
B7	Reference group	2.46	0	2.46	60	
	Experimental group	0.5	0.50	1.00	84	96.0
B8	Reference group	2.46	0	2.46	52	
	Experimental group	0.5	0.50	1.00	80	92.3
B9	Reference group	2.46	0	2.46	52	
	Experimental group	0.5	0.60	1.10	89	100

Except for groups B1 and B2, the amount of added fluorite in the experimental group was only about 20% of that in the reference group. With added boric acid, the total amount of mineralizer was still less than the amount of fluorite mineralizer in the reference group. The reduced amount of fluorite in the mineralizer directly reduces the fluorine emission and relieves stress on the environmental pollution.

The oversize rate of magnesium slag refers to the ratio between the weight of slag that remained on the sieve and the total weight of magnesium slag after the magnesium slag was passed through a 0.45 mm sieve (the weight of remaining Mg slag/total weight of Mg slag). The oversize rate is the numerical data used to measure the degree of pulverization of magnesium slag. In Table 4.8, the oversize rates of all of the reference groups are lower than those of the corresponding experimental groups, and this indicates that the magnesium slag in the experimental group has better volume stability. Figure 4.23 shows photos of magnesium slag in the reference group and in the boric acid-doping experimental groups after they were stored for a period of time. In panel (a), the magnesium slag was completely powdered, and in panel (b), the magnesium slag remained lumpy.

**Experiment II: using rare earth oxides to replace fluorite.** The raw materials used in Experiment II were exactly the same as those used in Experiment I. Different rare earth oxides (cerium oxide ( $\text{CeO}_2$ ), lanthanum oxide ( $\text{La}_2\text{O}_3$ ), neodymium oxide ( $\text{Nd}_2\text{O}_3$ ), yttrium oxide ( $\text{Y}_2\text{O}_3$ ), and terbium oxide ( $\text{Tb}_2\text{O}_3$ )) were used as mineralizers to replace fluorite. The experimental process was also the same as before. The

**Table 4.8** Formula for the industrial fluorine-free magnesium smelting test

Number of test 编号	Dolomite (kg)	Ferrosilicon (kg)	Fluorite (kg)	Type of mineralizer	Amount of mineralizer (%)
1	100	20.5	0	Boric acid	0.8
2	100	20.5	1.2	Boric acid	1.8
3	100	20.5	0	$\text{CeO}_2$ waste	0.8
4	100	20.5	1.2	$\text{CeO}_2$ waste	1.8

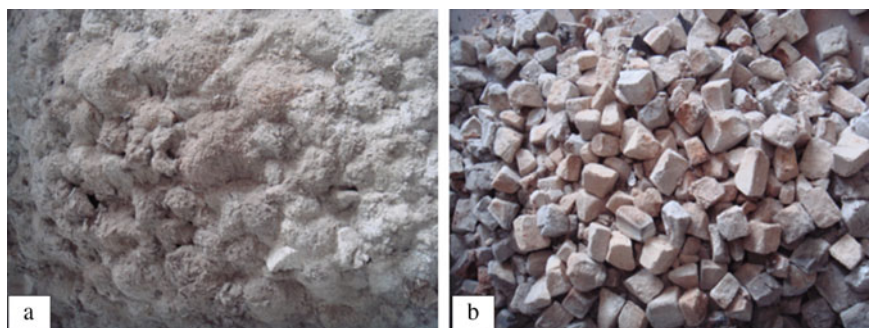


**Fig. 4.23** Morphology of Mg slag after the smelting experiment: **a** reference group using fluorite **b** experimental group using boric acid

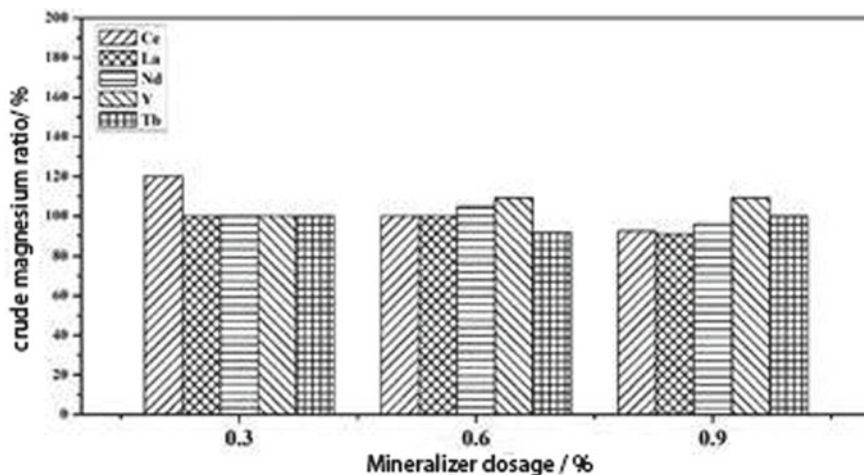


Fig. 4.24 Crude Mg yield of magnesium smelting using rare earth oxides as mineralizers

results indicate that when a rare earth oxide was used as a mineralizer in magnesium smelting, both the crude magnesium yield and the quality of crude magnesium were not inferior to that obtained using a fluorite mineralizer; also, the volume stability of magnesium slag was enhanced, and no powdering occurred. The crude magnesium ratios in the magnesium smelting experiments that used several rare earth oxides are shown in Fig. 4.24. In the figure, Ce, La, Nd, Tb, and Y denote  $\text{CeO}_2$ ,  $\text{La}_2\text{O}_3$ ,  $\text{Nd}_2\text{O}_3$ ,  $\text{Y}_2\text{O}_3$ , and  $\text{Tb}_2\text{O}_3$ , respectively. The amount of mineralizer on the abscissa refers to the weight percent of the added rare earth mineralizer in the raw materials.

As seen in Fig. 4.24, when the amount of added rare earth mineralizer was 0.3% of the total weight of the raw materials, the yields of crude magnesium in the experiment samples with rare earth oxides were 100% of that of the sample with fluorite mineralizer, except for  $\text{CeO}_2$ .  $\text{CeO}_2$  is a particularly prominent mineralizer used in magnesium smelting, and results in a crude magnesium ratio of 120%. Meanwhile, the amount of fluorite in the reference group was 2.5% of the total amount of raw materials, and this is times higher than that of a rare earth mineralizer. When the amount of added mineralizer was 0.6%,  $\text{CeO}_2$  and  $\text{Y}_2\text{O}_3$  showed greater advantages, and the corresponding crude magnesium yields were 105% and 109%, respectively. The crude magnesium rates of the remaining samples that used rare earth oxides also reached 100%, except for  $\text{Tb}_2\text{O}_3$  which was only 92%. When the amount of added mineralizer was 0.9%,  $\text{Y}_2\text{O}_3$  still maintained better performance with a crude magnesium yield of 109% whereas those of other rare earth oxides were not as good as that of the reference group, which used fluorite mineralizer. In the magnesium smelting experiment using rare earth oxides to replace fluorite as a mineralizer, the oversize rate of magnesium slag was consistent with the result of Experiment I; that is, when rare earth oxides were used as mineralizers, magnesium slag showed good

volume stability. However, for the reference sample that used fluorite as a mineralizer, the magnesium slag was instantly efflorescence when it was removed from the furnace.

Although a variety of rare earth oxides as mineralizers exhibit good effects in magnesium smelting, it is not practical to use them in large-scale production because of their high prices. However, the recycled waste of a CeO<sub>2</sub> polishing agent, which is used as an abrasive for polishing optical glass, still contains many rare earth oxides. From the perspective of reducing the costs of raw materials and recycling industrial by-products, using recycled CeO<sub>2</sub> polishing agent as a mineralizer for magnesium smelting instead of using fluorite has attractive prospects. The following section introduces in detail a magnesium smelting experiment using recycled CeO<sub>2</sub> polishing agent instead of fluorite.

**Magnesium smelting experiment using recycled CeO<sub>2</sub> instead of fluorite.** In this experiment, the raw materials for magnesium smelting were the same as those in previous experiments. The mineralizer of the experimental group was recycled CeO<sub>2</sub> polishing agent (provided by Ganzhou Jinchengyuan New Material Co., Ltd.), and the mineralizer of the reference group was fluorite. The recycled cerium oxide polishing agent is denoted C2. Phase analysis shows that the composition of C2 is 32.58% rare earth oxides, 31% Al<sub>2</sub>O<sub>3</sub>, 18% SiO<sub>2</sub>, 5.73% MgO, 4.57% F, and 3.97% CaO. XRD data and particle size distribution results are shown in Fig. 4.25; panel (a) shows the phase analysis XRD data of C2, and panel (b) shows the particle size distribution of C2.

The experimental result for the case when C2 was used to replace fluorite is shown in Fig. 4.26. The abscissa is the ratio between the amount of added C2 in the experimental group and that of added fluorite in the reference group. The ordinate is

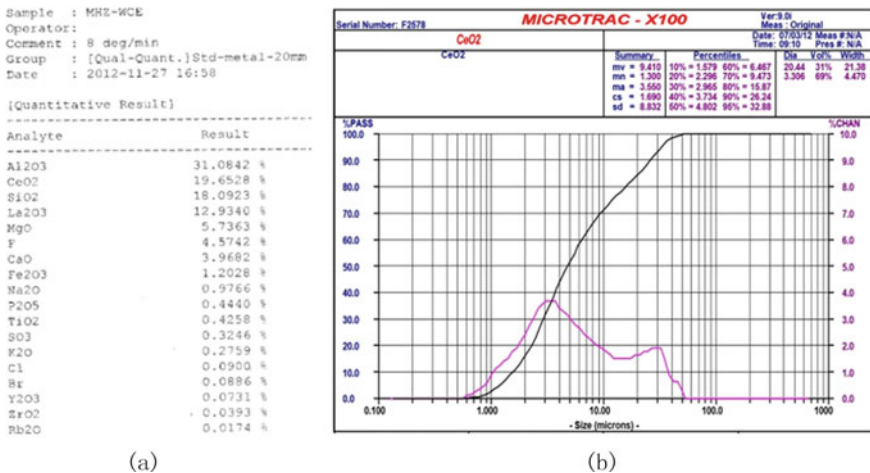
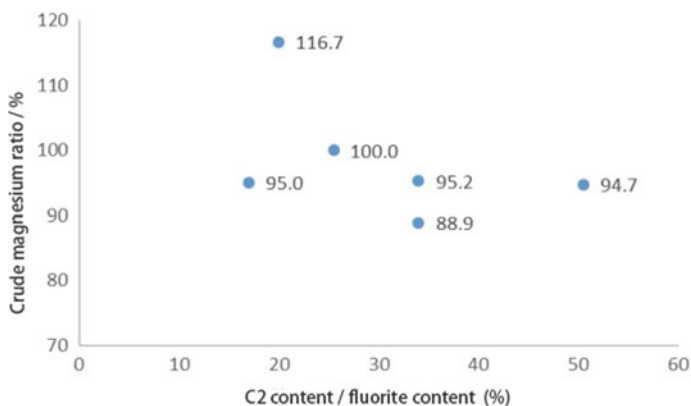


Fig. 4.25 Phase and particle size characterization of C2: a XRD data and b size distribution

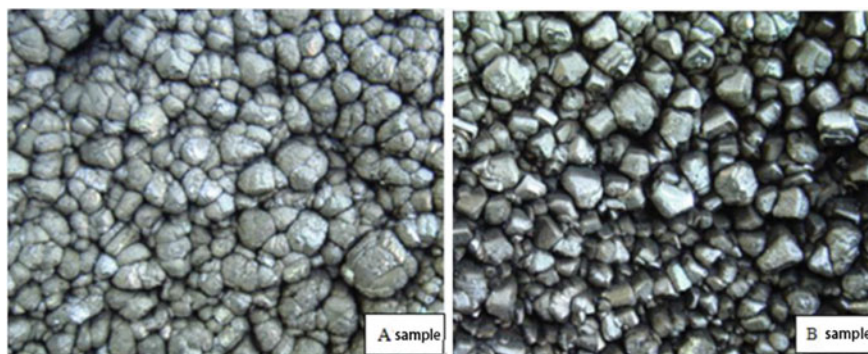


**Fig. 4.26** Magnesium smelting using C2

the ratio between the crude magnesium yield of the experimental group and that of the reference group.

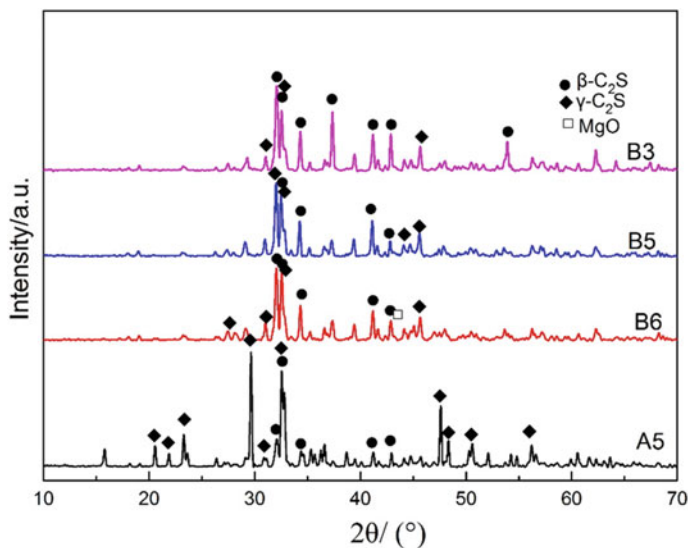
Figure 4.26 shows the results of the magnesium smelting experiment using C2 instead of fluorite. Compared with the results in Fig. 4.22 for the experiments that used boric acid to replace fluorite, it is clear that C2 is better than boric acid for use as a mineralizer in magnesium smelting. There are two sets of data that can meet or exceed the mineralizing effect of fluorite, and the amount of mineralizer was only 20–25% of the amount of fluorite. However, in industrial applications, a stable supply source of C2 needs to be further investigated. The morphology of the crude magnesium when recycled cerium oxide polishing agent was used as a mineralizer in magnesium smelting is shown in Fig. 4.27.

Figure 4.28 shows the XRD patterns of magnesium smelting slags with different amounts of added C2. The fluorite percent of the sample in the reference group



**Fig. 4.27** Morphology of crude magnesium from pilot experiment **a** reference group using fluorite **b** experimental group using C2





**Fig. 4.28** Comparison of XRD patterns for magnesium slag using C2

A was 2 wt%, and that of C2 in experimental groups B3, B5, and B6 were 1.01, 0.68, and 0.51%, respectively. As seen from the comparison between the XRD phase analysis of the reference group A5 and the experimental groups B6, B5, and B3, the characteristic peaks of  $\gamma$ -C<sub>2</sub>S almost disappeared, and the characteristic peaks of  $\beta$ -C<sub>2</sub>S were significantly enhanced in the experimental groups. The changes show that the content of  $\gamma$ -C<sub>2</sub>S decreased, whereas the content of  $\beta$ -C<sub>2</sub>S correspondingly increased in magnesium slag when recycled cerium oxide was used as a mineralizer. The added amount of recycled cerium oxide in the experimental group B3 was the highest, at a value of 1.01%, which is still about half the amount of fluorite in the reference group. Correspondingly, the content of  $\beta$ -C<sub>2</sub>S in the magnesium slag of B3 was the highest, and this magnesium slag sample had the best stability.

In summary, this pilot magnesium smelting test confirmed that the output and quality of crude magnesium that were obtained were basically consistent whether recycled cerium oxide or fluorite was used as a mineralizer. When the amount of added recycled cerium oxide was varied from 0.5 wt% to 1.0 wt% of the raw materials, there was little effect on the output of crude magnesium, but there was a significant impact on the stability of the magnesium slag. The magnesium slag was fragile when the added amount was less than 0.5 wt%, whereas the stability of magnesium slag became good when the added amount was above 0.7 wt%. As seen from the XRD pattern, using C2 as a mineralizer can prevent the crystal phase transition from  $\beta$ -C<sub>2</sub>S to  $\gamma$ -C<sub>2</sub>S, which stabilizes the magnesium slag. From a comprehensive consideration of the output and the quality of crude magnesium, and stability of magnesium slag, it was found that the optimal effect was achieved when the amount of added C2 was 0.7-1 wt% of the total raw materials. Using C2 instead of CaF<sub>2</sub> in

magnesium smelting lays a good foundation for the industrial production of new clean magnesium smelting technologies and also achieves the reuse of rare earth waste; thus, this approach has promising application prospects in resource conservation and environmental protection.

#### 4.2.6 Industrialized Test of Fluorine-Free Mineralizer

On the basis of the pilot test, boric acid (industrial grade) and recycled cerium oxide polishing agent were selected as fluorine-free mineralizers to replace fluorite. Industrial tests were conducted at Ningxia Huiye Magnesium Group Co., Ltd. The industrial test was implemented in accordance with the standard Pidgeon process, which has a technological flow as follows: dolomite calcination, batching, powder making, pelleting, packaging (pellets in paper bags), smelting conducted in reduction furnace, crude magnesium collected and refined, ingot costing, quality analysis, and final products are packaged.

**Experimental formula:** The formulas for the industrial fluorine-free magnesium smelting test are shown in Table 4.8. The amounts of mineralizer that are shown in the table are the percent of mineralizer in the total raw materials

**Experimental process:** The batching process combined manual and automatic batching systems. The pelleting process was completed using a pelletizer at Huiye's Magnesium No. 1 Branch Plant No.1 workshop. **Reduction smelting** was carried out using the production reduction furnace at Huiye's Magnesium No. 1 Branch Plant. The main working conditions during the test include: reduction temperature, degree of vacuum, water temperature, and sintering time; these factors were all implemented in accordance with the present production process standards of Huiye Magnesium Group Co., Ltd. **Measurement of crude magnesium output:** The input-output rates of every experimental batch were measured, recorded, and calculated separately. **Quality analysis of refined magnesium ingots:** The experimental crude magnesium was transported to the refining workshop for refining, separated and the quality and composition of the product were analyzed. **Monitoring and analysis of reduction slag:** The experimental batch of magnesium slag was sampled separately to determine the oversize rate and the contents of various components in the slag.

**Experimental results:** The output and yield of a single retort in the test batch were basically the same as those of the normal production data. Through quality analysis of the magnesium ingot, it was found that the experimental ingot meets all of the quality specifications for the product and that the morphology of the magnesium slag is basically all granular without powdering. Compared with the slag that used fluorite as a mineralizer, the slag in this experiment greatly reduced dust pollution to the environment. Figure 4.29 shows the magnesium slag generated in the industrial test, where panel (a) shows the magnesium slag that used boric acid to replace fluorite and panel (b) shows the magnesium slag that used C2 to replace fluorite.

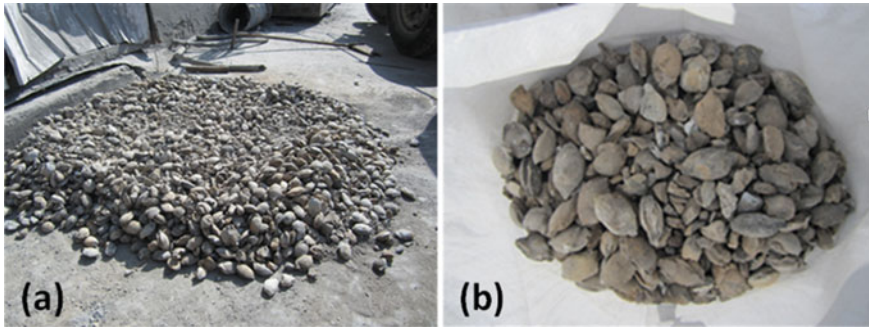


**Fig. 4.29** Morphology of magnesium slag after the industrial test: **a** using boric acid as a mineralizer and **b** using C2 as a mineralizer

### Conclusions:

The industrial test of fluorine-free magnesium smelting confirms that boric acid and C2 as fluorine-free mineralizers can be used to replace fluorite, which is usually used in magnesium smelting. This substitution can be made without affecting the output and production rate of magnesium products. The replacement does not change the original production process and does not increase the production costs. Furthermore, the stability of the slag is greatly enhanced, and so the problems of dust pollution during the collection, transport, and reuse of slag have been solved. More importantly, this approach reduces the use of fluoride from the natural sources and reduces fluoride pollution in soil, water, and air.

#### 4.2.7 Application of Fluorine-Free Mg Slag in Steel-Making

Using the fluorine-free magnesium slag to partially replace limestone as a slagging agent in steel-making reduces production costs, enables the recycling and use of industrial waste, and reduces the stress that magnesium slag has on the environment. Fluorine-free magnesium slag was first used to conduct a small laboratory test to confirm that there is no adverse effect on the quality of the simulated steel-making product, and then an industrial test was carried out in the steel plant.

Laboratory simulation experiments were carried out at the China Central Iron and Steel Research Institute [20]. Fluorine-free magnesium slag from the Heiyi magnesium Ltd. was used. This slag basically does not contain sulfur and phosphorus. The laboratory experiment uses low-S low-P iron, fluorine-free magnesium slag, and converter steel slag from the steelmaking production of Ningxia Steel as the raw materials. A certain ratio of magnesium slag and converter steel slag were mixed with iron powder, heated, melted, and held at a high temperature for a while to simulate converter steelmaking process and to investigate the change of sulfur and phosphorus content in iron-containing materials. **Experimental formula:** The

experimental materials included iron material and 10 wt% slags (steel slag + magnesium slag). 5, 10, 15, and 20% of the total slag of fluorine-free magnesium slag were used separately with steel slag to study the effect that magnesium slag has on steel making. **Experimental process:** The mixed powder was kept at 1550 °C for 40 min. After the experiment, molten steel and slag were discharged from a crucible and cooled in the air. The contents of C, Si, Mn, P, and S in the iron material were analyzed. **Experimental results:** With an increase in amount of added magnesium slag, the S content in the steel sample decreased, and the P contents only increased slightly. When the magnesium slag was 15 and 20%, the P contents of the samples were basically the same as that of the original iron powder. The results indicate that magnesium slag has no adverse effects on the quality of molten steel, especially the S and P in molten steel when magnesium slag is used to replace some of the steel slag as the slagging agent (The replacement ratio of magnesium slag to steel slag was controlled to be within 20%). Since magnesium slag has lower melting point, partial replacement of the slagging agent by magnesium slag is beneficial to converter slagging and increases the melting rate of the steel-making slagging agent. Because of laboratory conditions, the actual production effect on site will be better than the laboratory results.

**Industrial test** A further production test was carried out under actual production conditions at the Ningxia Steel Plant. Test scheme: A separate hopper for magnesium slag was used. Magnesium slag was added simultaneously when the first batch of slagging agent was added using the feeding platform. The amounts of added magnesium slag are 5, 10, 15, and 20%. In the first batch, there were three furnace tests: (1) Slagging agent was added according to normal steel-making production, and an additional 10% magnesium slag was added simultaneously when the first batch of slagging agent was added. (2) The amount of steel-making slagging agent was decreased by 10%, and 10% magnesium slag was added instead of the slagging agent. (3) The steel-making slagging agent was reduced by 20%, and 20% magnesium slag was used instead of the slagging agent. The experimental results indicate that without changing the present process conditions, magnesium slag can be used to partially replace lime as a slagging agent in steel making and that doing so has no negative impact on the quality of the finished steel products until the amount of substituted magnesium slag reaches 15%. In the second batch, the maximum percent of substituted magnesium slag was as high as 30%, and the effect was the same.

## References

1. Kim YJ, Nettleship I, Kriven W et al (1992) Phase transformations in dicalcium silicate: II, TEM studies of crystallography, microstructure, and mechanisms. *J Amer Ceram Soc* 75(9):2407–2419
2. Akira S, Yoshio A et al (1986) Development of dusting prevention stabilizer of stainless steel slag. *Kawasaki Steel Giho* 18:20–24
3. Chan C, Kriven WM et al (1992) Physical stabilization of the  $\beta \rightarrow \gamma$  transformation in dicalcium silicate. *J Am Ceram Soc* 75(6):1621–1627

4. Yang Q et al (2008) Stabilization of EAF slag for use as construction material. In: REWAS 2008: global symposium on recycling, waste treatment. Minerals, Metals and Materials Society, pp 49–54
5. Tossavainen M, Engström F et al (2007) Characteristics of steel slag under different cooling conditions. *Waste Manage* 27(10):1335–1344
6. Jiang H, Li L et al (2012) Study on aging phase transformation and property of air-quenching steel slag. *Bullet Chinese Ceramic Soc* 31(01):171–174 + 192
7. Zhu G (2014) Research on methods to suppress the expansion of steel slags and road performance used as roadbed filling material. Dissertation, Nanjing Forestry University
8. Cui Z, Ni X et al (2006) Study on the expansibility of magnesium slag. *Fly ash Compreh Utilization* 06:8–11
9. Jürgen G (2000) Properties of iron and steel slags regarding their use. In: Paper presented at the 6th international conference on molten slags, fluxes and salts, Stockholm City, Stockholm, Sweden-Helsinki, Finland, 12–17 June
10. Du C, Wu L et al (2012). Dust pollution prevention of magnesium slag. In: Paper presented at the 8th conference of Chinese society of particuology, Sept 5–8, Hangzhou, China
11. Wu L, Yang Q, Han F et al (2013) Dust control of magnesium production by Pidgeon process. In: Paper presented at the 7th international conference on micromechanics of granular media, Sydney, 8–12 July
12. Feng J, Long S et al (1985) Effect of minor ions on the stability of  $\beta$ -C<sub>2</sub>S and its mechanism. *J Chinese Ceramic Soc* 04:424–432
13. Zhang W, Zhang J et al (2019) Structure and activity of dicalcium silicate. *J Chinese Ceramic Soc* 47(11):1663–1669
14. Huang W, Wen Z et al (2018) Effects of phosphorus and sulfur doping on the crystal structure of dicalcium silicate. *Bulletin of the Chinese ceramic society* 37(08):2502–2505 + 2511
15. Han F, Yang Q et al (2013) Reclaim and treatment of magnesium slag from pidgeon process. *Inorgan Chem Indus* 45(7):52–55
16. Han F, Yang Q, Wu L et al (2011) Treatments of magnesium slag to recycle waste from pidgeon process. *Adv Mater Res* 418–420:1657–1667
17. Barua S, Wynnyckyj JR et al (1981) Kinetic of the silicothermic reduction of calcined dolomite in flowing hydrogen. *Can Metall Q* 20(3):295–306
18. Feng G et al (2009) Life cycle assessment of primary magnesium production using the pidgeon process in China. *Int J Life Cycle Assess* 14:480–489
19. Wu L, Han F, Hang Q et al (2012) Fluoride emissions from Pidgeon process for magnesium production. In: Paper presented at the 27th international conference on solid waste technology and management, Philadelphia, PA U.S.A, March 11–14
20. Han F etc (2012) National international science and technology cooperation. Study on the comprehensive treatment and recycling technology of magnesium slag(2010DFB50140)Project Technical Report

**Open Access** This chapter is licensed under the terms of the Creative Commons Attribution-NonCommercial-NoDerivatives 4.0 International License (<http://creativecommons.org/licenses/by-nc-nd/4.0/>), which permits any noncommercial use, sharing, distribution and reproduction in any medium or format, as long as you give appropriate credit to the original author(s) and the source, provide a link to the Creative Commons license and indicate if you modified the licensed material. You do not have permission under this license to share adapted material derived from this chapter or parts of it.

The images or other third party material in this chapter are included in the chapter's Creative Commons license, unless indicated otherwise in a credit line to the material. If material is not included in the chapter's Creative Commons license and your intended use is not permitted by statutory regulation or exceeds the permitted use, you will need to obtain permission directly from the copyright holder.

